Cancer Letters 451 (2019) 100–109

Contents lists available at ScienceDirect

Cancer Letters

journal homepage: www.elsevier.com/locate/canlet

Original Articles

Forced expression of DYRK2 exerts anti-tumor effects via apoptotic induction in liver cancer

Shiho Yokoyama-Mashima[a,b], Satomi Yogosawa[a], Yumi Kanegae[c], Shinichi Hirooka[d], Saishu Yoshida[a], Takashi Horiuchi[e], Toya Ohashi[f], Katsuhiko Yanaga[e], Masayuki Saruta[b], Tsunekazu Oikawa[b], Kiyotsugu Yoshida[a,*]

[a] Department of Biochemistry, The Jikei University School of Medicine, Tokyo, Japan
[b] Department of Gastroenterology and Hepatology, The Jikei University School of Medicine, Tokyo, Japan
[c] Core Research Facilities for Basic Science (Division of Molecular Genetics), Research Center for Medical Science, The Jikei University School of Medicine, Tokyo, Japan
[d] Department of Pathology, The Jikei University School of Medicine, Tokyo, Japan
[e] Department of Surgery, The Jikei University School of Medicine, Tokyo, Japan
[f] Division of Gene Therapy, Research Center for Medical Science, The Jikei University School of Medicine, Tokyo, Japan

ARTICLE INFO

Keywords:
DYRK2
Liver cancer
Adenovirus
Proliferation
Apoptosis

ABSTRACT

Liver cancer is highly aggressive and globally exhibits a poor prognosis. Therefore, the identification of novel molecules that can become targets for future therapies is urgently required. We have reported that dual-specificity tyrosine-regulated kinase 2 (DYRK2) functions as a tumor suppressor by regulating cell survival, differentiation, proliferation and apoptosis. However, the research into its clinical application as a molecular target has remained to be explored. Here we showed that DYRK2 knockdown enhanced tumor growth of liver cancer cells. Conversely and more importantly, adenovirus-mediated overexpression of DYRK2 resulted in inhibition of cell proliferation and tumor growth, and induction of apoptosis both *in vitro* and *in vivo*. Furthermore, we found that liver cancer patients with low DYRK2 expression had a significantly shorter overall survival. Given the findings that DYRK2 regulates proliferation and apoptosis of cancer cells, DYRK2 expression could be a promising predictive marker of the prognosis in liver cancer. Stabilized or forced expression of DYRK2 may become thus a potential target for novel gene therapy against liver cancer.

1. Introduction

Liver cancer is the second frequent tumor worldwide and is associated with a poor prognosis [1]. The pathogenesis of liver cancer is frequently linked to genomic alterations influenced by chronic viral infection, alcohol consumption, toxin ingestion and metabolic stress [2–4]. For the treatment of liver cancer, surgical resection, radiofrequency ablation (RFA) and liver transplantation for patients with early-stage, and transcatheter arterial chemoembolization (TACE) for those with intermediate-stage are currently available and have shown some efficacy. However, patients with vascular invasion and distant metastasis have a poor prognosis. Recently, tyrosine kinase inhibitors, including sorafenib, lenvatinib and regorafenib, have been developed and approved for clinical use against advanced cancer patients, but their effects are limited [5–9]. It is therefore urgently required to develop new therapeutic option against liver cancer.

Dual-specificity tyrosine-regulated kinase 2 (DYRK2) is a protein kinase that phosphorylates its substrates at serine and threonine residues. Initially, DYRK2 was found to phosphorylate p53 at Ser46 to regulate apoptotic cell death in response to DNA damage [10]. DYRK2 is ubiquitinated by E3 ligases such as MDM2 and SIAH2, for its constitutive degradation and impaired DYRK2-mediated phosphorylation of p53 at Ser46 [11,12]. In response to genotoxic stress, DYRK2 is phosphorylated at Thr33 and Ser369 by ataxia-telangiectasia mutated (ATM) to be stabilized by inhibiting MDM2-mediated degradation, which induces the kinase activity toward p53 at Ser46 in the nucleus [12]. Knockdown of DYRK2 increases cell proliferation and tumor progression *in vivo* through the escape of c-Jun and c-Myc from ubiquitination-mediated degradation in breast cancer cells [13]. In addition, we have previously showed that DYRK2 plays an important role in epithelial-mesenchymal transition (EMT) by degrading Snail and stabilizing E-cadherin in breast cancer cells [14]; DYRK2 also regulates chemosensitivity through snail degradation in ovarian serous adenocarcinoma [15]. It has also been reported that the expression of DYRK2

* Corresponding author. Department of Biochemistry, The Jikei University School of Medicine, 3-25-8, Nishi-shinbashi, Minato-ku, Tokyo, 105-8461, Japan.
E-mail address: kyoshida@jikei.ac.jp (K. Yoshida).

https://doi.org/10.1016/j.canlet.2019.02.046
Received 2 November 2018; Received in revised form 10 January 2019; Accepted 19 February 2019

protein is controlled by ubiquitination-mediated proteasomal degradation and is downregulated in various human cancer tissues [16]. Recent genome-wide association studies have also shown that the somatic mutation of DYRK2 correlates with breast cancer risk [17]. These findings collectively support the idea that DYRK2 functions in tumor suppression against liver cancer. However, the mechanisms underlying the effects of DYRK2 on the *in vivo* proliferative capacity, cell cycle distribution, apoptosis, and tumorigenicity in liver cancer are largely unclear. The present study aimed to explore the mechanisms underlying the effects of DYRK2 in liver cancer.

2. Materials and methods

2.1. Cell culture

The human liver cancer cell lines HuH1, HLE, HLF, PLC/PRF5 and SK-Hep1 were obtained from the JCRB Cell Bank or the ATCC. HuH7 was obtained from the RIKEN. Cells were cultured in Dulbecco's modified Eagle's medium (DMEM) with 10% fetal bovine serum (FBS) and 1% penicillin-streptomycin (Nacalai Tesque). All cell lines were maintained at 37 °C in a 5% CO_2 incubator.

2.2. Plasmid transfection and virus transduction

The near-infrared fluorescent protein 720 (iRFP720) sequence was amplified from piRFP720-N1 (Addgene) using the primer sequences listed in Supplementary Table S3 as described previously [18]. The amplified product was inserted into a FG12 lentiviral vector [19] and the modified plasmid was transfected into 293T cells using polyethyleneimine (PEI)-MAX (Polysciences Inc). The virus-containing supernatant was applied to HuH1 cells with 10 μg/ml polybrene (Sigma-Aldrich). A stable HuH1 cell line expressing iRFP720, named iRFP720-HuH1, was established by sorting positive cells with a MoFlo XDP cell sorter. To generate two different stable short hairpin RNA (shRNA)-DYRK2 cell lines, shRNAs against non-specific effects, luciferase (shLuc) or DYRK2 (Supplementary Table S4) were cloned into a pSUPER-puro-vector and subsequences were inserted into a FG12 lentiviral vector. The plasmid was introduced into 293T cells, as described above, and the supernatant was applied to HuH1and PLC/PRF5 cells with 10 μg/ml polybrene. The resulting stable cell lines were designated as iRFP720-HuH1/shDYRK2 #1 and #5, and PLC/PRF5shDYRK2 #1 and #5.

2.3. Adenovirus vector and cell transfection

Since it was impossible to produce adenovirus directly expressing DYRK2 from the EF1α promoter by uncertain reason, adenovirus vectors (Adv) expressing Flag-DYRK2 were designed to depend upon Cre expression. Flag-DYRK2 and Flag-DYRK2KR as described previously [13,14] were inserted into the SwaI site of pAxEFLNLwi2, which was the cosmid cassette for pAxEFNCre-dependent expression Adv construction [20]. pAxEFLNLfDYRK2it2 and pAxEFLNLfDYRK2KRit2 had neomycin-resistant genes flanked by two loxPs in front of these expression units as stuffers. Ad-DYRK2 and Ad-DYRK2KR were generated as described previously [21]. Ax1w1, which bears no insert, was used as a control (hereafter “Ad-1w1”) [22]. The Ad-Cre-carrying Cre expression unit under control of the EF1alpha promoter was previously described [23]. Advs were titrated via the previously reported method [24].

2.4. Quantitative real-time polymerase chain reaction (PCR) analyses

Total RNA was isolated using TRIsure (Nippon Genetics). cDNA was synthesized from total RNA using RevatraAce reverse transcriptase (Toyobo) and oligonucleotides or random primers. Quantitative real-time PCR was performed using the primer sequences listed in Supplementary Table S3 and PicoReal96 (Thermo Fisher Scientific).

2.5. Immunoblotting

Immunoblot analyses were carried out as previously described [14,15] using antibodies against DYRK2 (Sigma-Aldrich), c-Myc, cyclin D1, cyclin D2 and p53 (Santa Cruz Biotechnology), phospho-p53-Ser46 (Bio Academia) or tubulin (Sigma-Aldrich). The dilution method is all 1:1000.

2.6. Cell growth assay

A CCK-8 cell growth assay was performed in triplicate using the Cell Counting Kit-8 assay (Dojindo Laboratory) according to the manufacturers' instructions. In a colony formation assay, cells were plated into 6-well culture plates and cultured for 8 days to allow colony formation, as described previously [25].

2.7. Cell cycle analyses

Cells were harvested at the suitable time and fixed in 70% ethanol overnight at −20 °C, after which they were incubated with 100 μg/ml RNase and propidium iodide (40 μg/mL PI; Sigma-Aldrich) in FACS buffer for 30 min at 37 °C. The data were acquired from a MACS Quant flow cytometer (Miltenyi Biotec) and analyzed using the FlowJo software program (FlowJo LLC Ashland).

2.8. Apoptosis assay

Cells were washed with chilled PBS, resuspended in 100 μL of Binding Buffer, and incubated with Annexin V-FITC (BD Transduction Laboratories) and 7-AAD (eBioscience) for 15 min at 4 °C in the dark, according to the manufacturer's instructions. The cells were analyzed using a MACS Quant flow cytometer.

2.9. Animal studies and in vivo imaging

Our animal experiment protocol was approved by the Institutional Animal Care and Use Committee of Jikei University (No. 2015-069, 2017-038), and the studies were performed in accordance with the Guidelines for the Proper Conduct of Animal Experiments of the Science Council of Japan. For subcutaneous space injections, 6-week-old male nude mice (BALB/cA Jcl-nu/nu; CLEA) were injected with 3×10^6 cells of each of the cell lines stably expressing shRNA or luciferase. Four weeks after implantation, the tumor was monitored using the IVIS Lumina *in vivo* imaging system (Perkin Elmer). Tumor volumes were calculated according to the following formula: V (mm^3) = 0.5 × (larger diameter × smaller $diameter^2$).

2.10. Mouse xenografts and in vivo treatment with adenovirus

Mice were subcutaneously injected on one side with iRFP720-HuH1 cells (2×10^6 cells per mouse). Two weeks after injection, mice with too big or too small tumors were excluded, and the rest of the mice were randomly divided into three equal groups: Ad-DYRK2, Ad-DYRK2KR and empty viruses as control. In each group, the mice received multisite intratumor injections of the corresponding recombinant virus at 1×10^9 plaque-forming units (pfu)/mouse through single injections. The tumor growth was evaluated based on the tumor size. Tumor samples were immunostained with hematoxylin and eosin (H&E), anti-ki67, anti-caspase-3 or terminal deoxynucleotidyl transferase dUTP nick end labeling (TUNEL).

2.11. Immunostaining

For immunostaining, excised xenografts were fixed with 4% paraformaldehyde and frozen. Frozen sections (7 μm thick) were stained using rabbit IgG against human Ki67 (dilution 1:250; Abcam) and

cleaved Caspase-3 (dilution 1:300, Cell Signaling Technology) overnight at 4 °C. For TUNEL staining, frozen sections were reacted using an *in situ* Apoptosis Detection Kit (Takara). The sections were observed under a BZ-9000 fluorescence microscope (Keyence). The number of stained cells was determined by counting the cells in five places with a field of view for 400 times.

2.12. Patient data

Sixty-seven primary liver cancer samples from surgically-treated patients obtained from the Jikei University Hospital between 2009 and 2012 were analyzed. The Jikei University School of Medicine Ethics Review Committee approved the study protocol (No.29-038). Informed consent has been obtained via disclosing information, along with specification that coded or anonymous leftover material is used for research and patients have been offered the option to opt out. Immunostaining samples were histologically diagnosed with liver cancer by H&E staining. All samples were treated under the guidelines and used for immunohistochemical (IHC) staining reactions with antibody to DYRK2 (1:200; Sigma). For the DYRK2 expression, the cytoplasmic staining intensity was scored semiquantitatively using an overall intensity score with four categories: IHC score 0, negative staining; 1, weak staining; 2, moderate staining; and 3, strong staining (Supplementary Fig. S5). According to above classification, the samples were then divided into two groups: a high-expression group (including the moderate and strong categories) and a low-expression group (including the negative and weak categories).

2.13. Statistical analyses

Data are presented as the mean ± standard deviation (SD). Group comparisons were performed using the parametric Student's *t*-test. Differences with $p < 0.05$ were considered significant. The overall survival time was censored at the time of the last follow-up or death. The calculation of the overall survival was initiated on the date of surgery. Statistical analyses were performed using the Stata software program, release 14 (Stata Corp. LP). The relationship between the clinicopathological factors and staining findings were analyzed by the Chi-squared test or Fisher's exact test. Furthermore, to analyze the patients' survival among different DYRK2 profiles, we divided the patients into two groups and investigated the clinical stage. The survival was analyzed using the Kaplan–Meier method and evaluated by the log–rank test. P-values < 0.05 were considered statistically significant.

3. Results

3.1. Downregulation of DYRK2 enhances proliferation and cell cycle in liver cancer cells

Liver cancer cell lines can be classified as epithelial- and mesenchymal-types, in which the latter is much more aggressive with poorly differentiated phenotype than the former [26]. We have shown that DYRK2 regulates Snail degradation in a kinase-dependent manner and that the decreased expression of DYRK2 in breast cancer promotes invasion and distant metastasis via EMT [14]. There is accumulating evidence that the DYRK2 expression is inversely correlated with cancer malignancy and the prognosis [14,16,27,28].

We evaluated the expression levels of DYRK2 in epithelial (HuH1, HuH7, Hep3B, PLC/PRF5) and mesenchymal liver cancer cells (SK-Hep1, HLE, HLF). DYRK2 expression in epithelial cancer cells was markedly higher than that in mesenchymal cancer cells (Fig. 1A), suggesting that DYRK2 expression is low in liver cancer cells with highly aggressive potentials. To evaluate the association between the DYRK2 expression and the proliferation, we stably knocked down DYRK2 in HuH1 and PLC/PRF5 cells (shRNA-DYRK2 cells) (Fig. 1B, Supplementary Fig. S1A). We have previously reported that c-Myc was suppressed by DYRK2 in a kinase activity-dependent manner in breast cancer cells, indicating its role for suppressing proliferation and G1-S phase transition in the cell cycle [13]. Similarly, knockdown of DYRK2 led to the accumulation of c-Myc, Cyclin D1 and Cyclin D2 in HuH1 and PLC/PRF5 (Fig. 1B, Supplementary Fig. S1A). In concert with this finding, the proliferation was increased in cells with DYRK2 knockdown compared to those with control shRNA (Fig. 1C and D, Supplementary Fig. S1B). Cell cycle analyses using the flow cytometry showed that DYRK2 knockdown cells reduced the G1 population and increased the S-phase cell fractions compared with control cells (Fig. 1E, Supplementary Fig. S1C). These results indicate that knockdown of DYRK2 accelerates cell proliferation in liver cancer cells.

3.2. Downregulation of DYRK2 enhances tumor growth in vivo

To investigate the role of DYRK2 in tumor growth of liver cancer cells *in vivo*, we explored the effects of DYRK2 knockdown in a liver cancer xenograft model. HuH1 and PLC/PRF5 cells transduced with shLuc or shDYRK2 were inoculated into the subcutaneous space of male nude mice. At 4 weeks after inoculation, tumors derived from DYRK2-knockdown liver cancer cells were significantly larger than those from control cells (Fig. 2A–C, Supplementary Figs. S2A and B). The tumor weights were remarkably higher than those with control cells (Fig. 2D, Supplementary Fig. S2C). These results suggest that down-regulating DYRK2 expression enhanced tumor growth of liver cancer cells *in vivo*.

3.3. Infection of Ad-DYRK2 in liver cancer cells inhibits growth and induces apoptosis in vitro

The expression of DYRK2 in normal human hepatocytes was markedly higher than that in liver cancer cell lines (Supplementary Fig. S3A). This finding led us to have an idea that overexpression of DYRK2 in cancer cells could exert an anti-tumor effect. Therefore, we decided to conduct an experiment by the overexpression of DYRK2 using adenovirus (Ad-DYRK2). HuH1 cells were infected with Ad-DYRK2 or Ad-empty vector (Adv) as a control at MOIs of 50, 100, and 200. The cell proliferation ability of Ad-DYRK2 was markedly decreased in a dose-dependent manner compared with control cells (Supplementary Figs. S3B–D), and 100 MOI was determined as the optimal dose without the cell toxicity.

To evaluate the effect of DYRK2 on cell proliferation and apoptosis in liver cancer, we generated HuH1 cells or PLC/PRF5 cells that transiently expressed DYRK2 (Ad-DYRK2), kinase-dead DYRK2 mutant (K178R) of Ad-DYRK2 (Ad-DYRK2-KR) or Adv control [13,14]. As expected, overexpression of DYRK2 reduced the levels of c-Myc, Cyclin D1 and Cyclin D2 (Fig. 3A). Next, the cell proliferation in Adv, Ad-DYRK2 or Ad-DYRK2-KR transduced cells was evaluated by CCK-8 assay. A significant inhibition of tumor growth in Ad-DYRK2 cells but not Ad-DYRK2-KR cells was observed (Fig. 3B). Comparable result was obtained with the colony formation assay (Supplementary Fig. S3E). We further investigated the effect of augmented DYRK2 on the cell cycle progression. Overexpression of DYRK2 was associated with increase of the G1 population and decrease of the S-phase and G2 populations compared with control or Ad-DYRK2-KR cells (Fig. 3C). These findings collectively indicate that overexpression of DYRK2 inhibits cell proliferation and cell cycle progression in a kinase activity-dependent manner.

We previously demonstrated that DYRK2 induces p53AIP1 expression and apoptosis in a p53-Ser46 phosphorylation-dependent manner [10]. Indeed, overexpression of DYRK2 induced Ser46 phosphorylation in liver cancer cells (Fig. 3D). To confirm the involvement of forced-expression of DYRK2 on apoptosis, we assessed the apoptotic rate using a flow cytometric analysis. The number of Anexin-V+/7-AAD+, Anexin-V+/7-ADD- cells was increased in Ad-DYRK2 cells but not Ad-DYRK2-KR cells (Fig. 3E). These data indicate that overexpression of DYRK2 elicits early to end stage apoptosis in a kinase-dependent

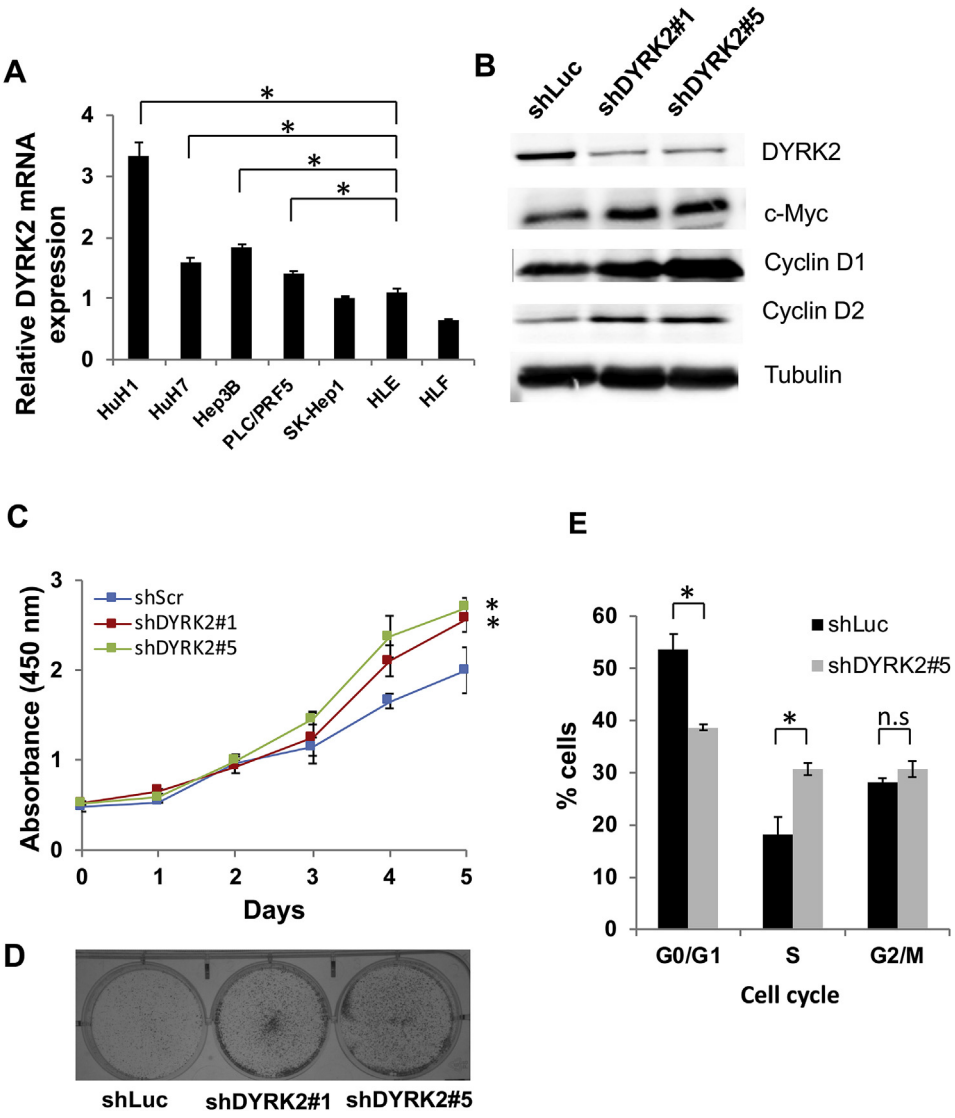

Fig. 1. Stable knockdown of DYRK2 enhanced cell proliferation activity in HuH1 human liver cancer cells. (A) Representative quantitative RT-PCR showed that the DYRK2 mRNA expression in epithelial cell lines (HuH1, HuH7, Hep3B, PLC/PRF5) was higher than that in mesenchymal cell lines (SK-Hep1, HLE, HLF) (*$p < 0.01$). (B) HuH1 cells were stably infected with lentivirus encoding shDYRK2#1, shDYRK2#5 or shLuc as control. The expression of DYRK2, c-Myc, Cyclin D1 and Cyclin D2 was analyzed by Western blotting. (C) Association between DYRK2 expression and cell proliferation of liver cancer. Cell growth was measured by the CCK-8 assay. Data are presented as the mean ± SD (n = 3; *$p < 0.05$). (D) Cell growth was measured by the colony formation assay. (E) Cells were stained with propidium iodide, and the cell cycle was analyzed using flow cytometry (*$p < 0.01$).

manner.

3.4. Anti-tumor effect induced by Ad-DYRK2 in a xenograft model

To extend these findings *in vivo*, we examined the oncolytic potential of Ad-DYRK2 in HuH1 cells using xenograft tumors. HuH1 cells were transplanted subcutaneously into nude mice, which were divided into 3 groups when tumor volumes reached approximately 150 mm^3. Adv, Ad-DYRK2 or Ad-DYRK2-KR cells (1×10^9 pfu) were then inoculated into the tumor. A whole-body imaging was performed by *in vivo* imaging system (IVIS) before and after injection of adenovirus (Fig. 4A), and the tumor size was monitored at the same time (Fig. 4B and C). At 3 weeks after injection, the tumor formation derived from Ad-DYRK2 cells was significantly smaller than that in the Adv or Ad-DYRK2-KR groups (Fig. 4B–D). Consistently, the tumor weights derived from Ad-DYRK2 cells were lower than those in other groups (Fig. 4D). These findings indicate that the infection of Ad-DYRK2 exerts anti-tumor effect *in vivo*. Immunohistochemical analyses showed that decreased expression of ki67 and increased expression of caspase-3 and TUNEL were observed in Ad-DYRK2 xenograft compared with the Adv or Ad-DYRK2-KR groups (Fig. 4E), supporting the conclusion that Ad-DYRK2 inhibited tumor growth and induced apoptosis in a kinase activity-dependent manner.

3.5. Expression of DYRK2 as a predictor of the outcome in liver cancer

We examined the DYRK2 expression in human liver cancer specimens and whether the levels were associated with over survival. Sixty-seven hepatocellular carcinoma (HCC) patients who underwent liver resection were enrolled in this study. We investigated the expression of DYRK2 in the tumor tissues and non-tumor tissues by immunohistochemical analyses. The expression of DYRK2 was down-regulated in the tumor tissues compared with the non-tumor tissues (Fig. 5A, Supplementary Table 5). In order to assess the correlations between DYRK2 expression and clinicopathologic parameters, the Chi-squared test was performed using our follow-up database (Supplementary Table 1). According to the classification as described in material and methods, the 67 patient tissues were divided into two groups with tumor regions and non-tumor regions. For non-tumor regions, there were 58 (86.6%) with high DYRK2 expression and 9 (13.4%) with low DYRK2 ($p < 0.001$). This finding demonstrated that DYRK2 expression is significantly high in non-tumor regions. By sharp contrast, for tumor regions, there were 28 (41.8%) with high DYRK2 expression and 39 (58.2%) with low DYRK2, suggesting that DYRK2 expression is substantially low in tumor-regions compared with that in non-tumor regions. More importantly, comparison of DYRK2 expression between tumor regions and non-tumor regions in each patient tissue (n = 67) demonstrated that DYRK2 expression in tumor regions was

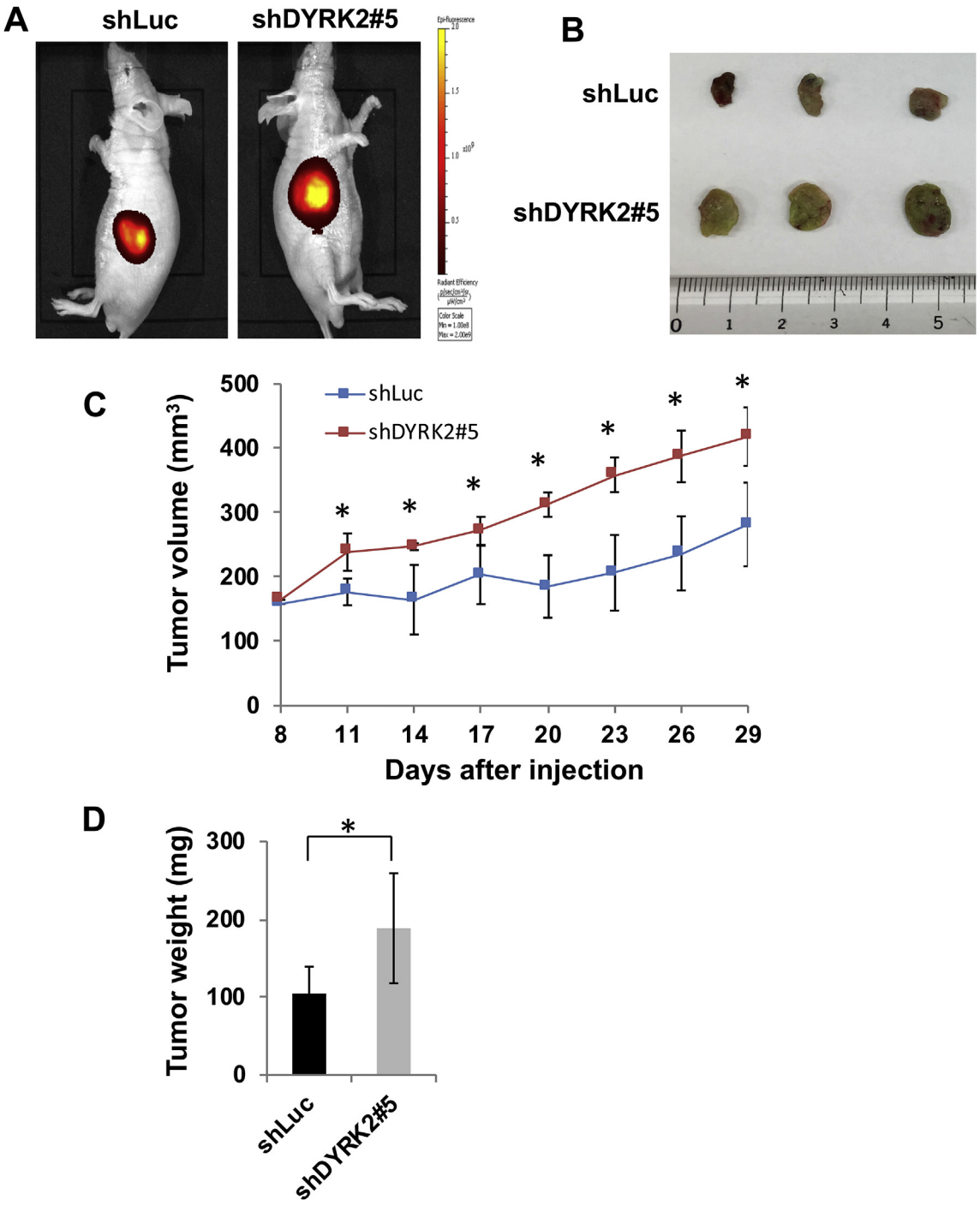

Fig. 2. DYRK2 knockdown increased cell growth *in vivo*. (A) IVIS luminescence images of the tumor in mice at four weeks after inoculation with iRFP720-labeled HuH1 cells. The color scale range is from 1×10^8 to 2×10^9 p/s/cm^2/sr. (B) Representative pictures of tumors taken four weeks after inoculation. (C) Tumor growth curves are plotted for shDYRK2 #5 and shLuc cells. Data are presented as the mean ± SD (shLuc n = 5, shDYRK2 n = 5; *P < 0.05). (D) The weight of the tumor at four weeks is shown. Data are presented as the mean ± SD (n = 5; *P < 0.05). (For interpretation of the references to color in this figure legend, the reader is referred to the Web version of this article.)

significantly lower than that in non-tumor regions (Supplementary Table 5). Liver cirrhosis was independently identified as a factor associated with DYRK2 expression ($p = 0.024$). In the multivariate analysis, DYRK2 expression was also retained as a significant and independent variable associated with overall survival. ($p = 0.01$; Supplementary Table 2). Indeed, a significant shorter survival was observed in HCC patients with low DYRK2 expression ($p = 0.0049$; Fig. 5B). These results support our hypothesis that the expression of DYRK2 could be a predictor of the outcome among patients with liver cancer.

4. Discussion

In this study, we showed that DYRK2 suppresses proliferation and promotes apoptosis in liver cancer cells. We have previously reported that DYRK2 silencing increased the cell proliferation in several human cancer cells (breast, ovarian and colorectal cancer) with impeding by code privation of c-Myc or c-Jun, and that DYRK2 induced p53AIP1 expression and apoptosis in a Ser46 phosphorylation-dependent manner [10,13]. However, the precise functional roles of DYRK2 in

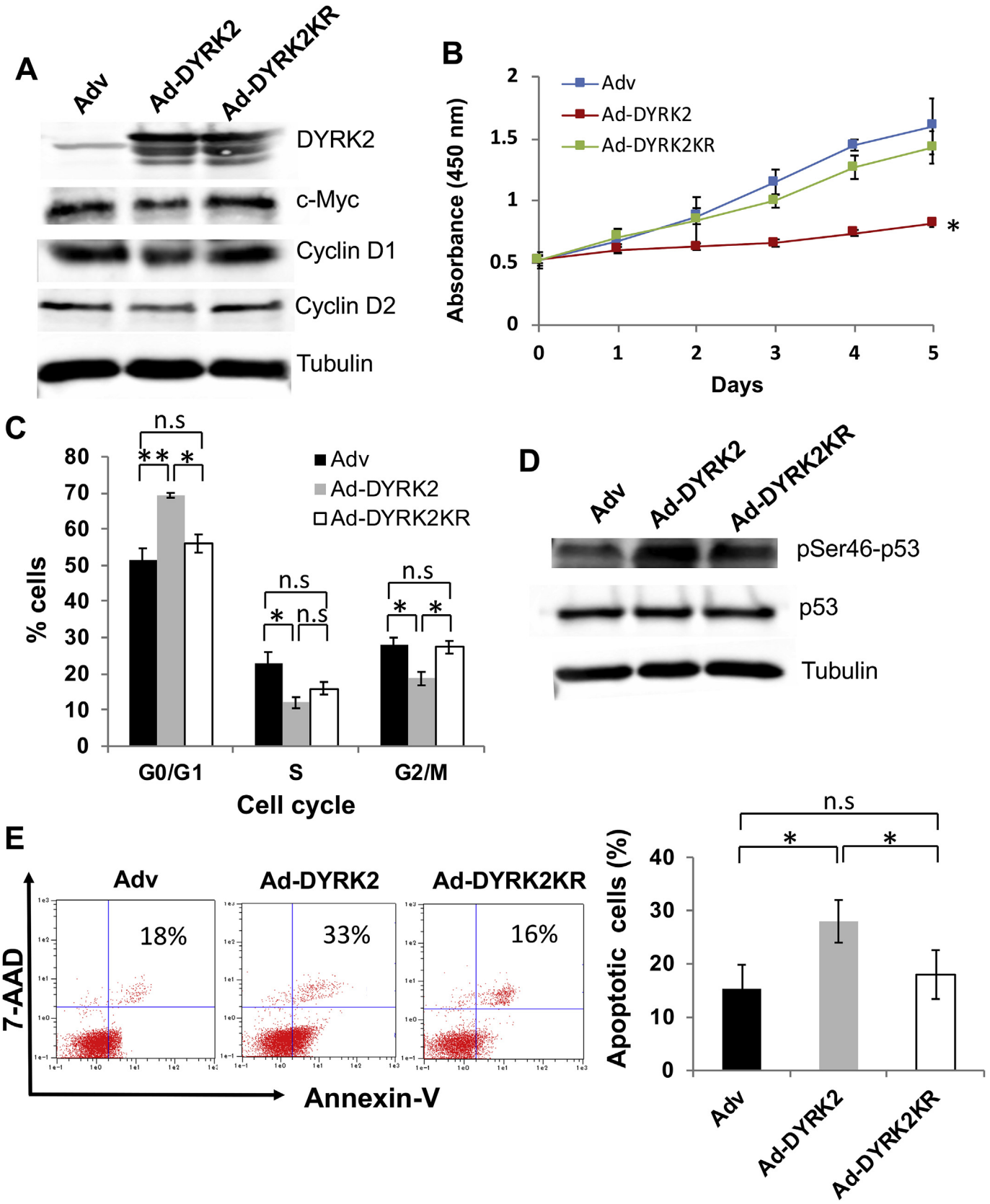

Fig. 3. Overexpression of DYRK2 inhibited cell proliferation activity in HuH1 liver cancer cells. (A) HuH1 cells were infected with adenovirus encoding DYRK2 (Ad-DYRK2), kinase-dead mutant (K178R) of DYRK2 (Ad-DYRK2-KR) or empty vector (Adv) as control. The expression of DYRK2, c-Myc, Cyclin D1, and cyclin D2 was analyzed by Western blotting. (B) Association between the DYRK2 expression and cell proliferation of liver cancer. Cell growth was measured by the CCK-8 assay. Data are presented as the mean ± SD (n = 3; *p < 0.01). (C) Cells were stained with propidium iodide, and the cell cycle was analyzed using flow cytometry (*p < 0.05, **p < 0.01). (D) The expression of phospho-p53 (Ser46) and p53 was analyzed by Western blotting. (E) The ratio of apoptotic HuH1 cells expressing Ad-DYRK2, Ad-DYRK2-KR or Adv was analyzed by Annexin V-FITC/PI double staining. Data are presented as the mean ± SD from three independent experiments (*p < 0.05).

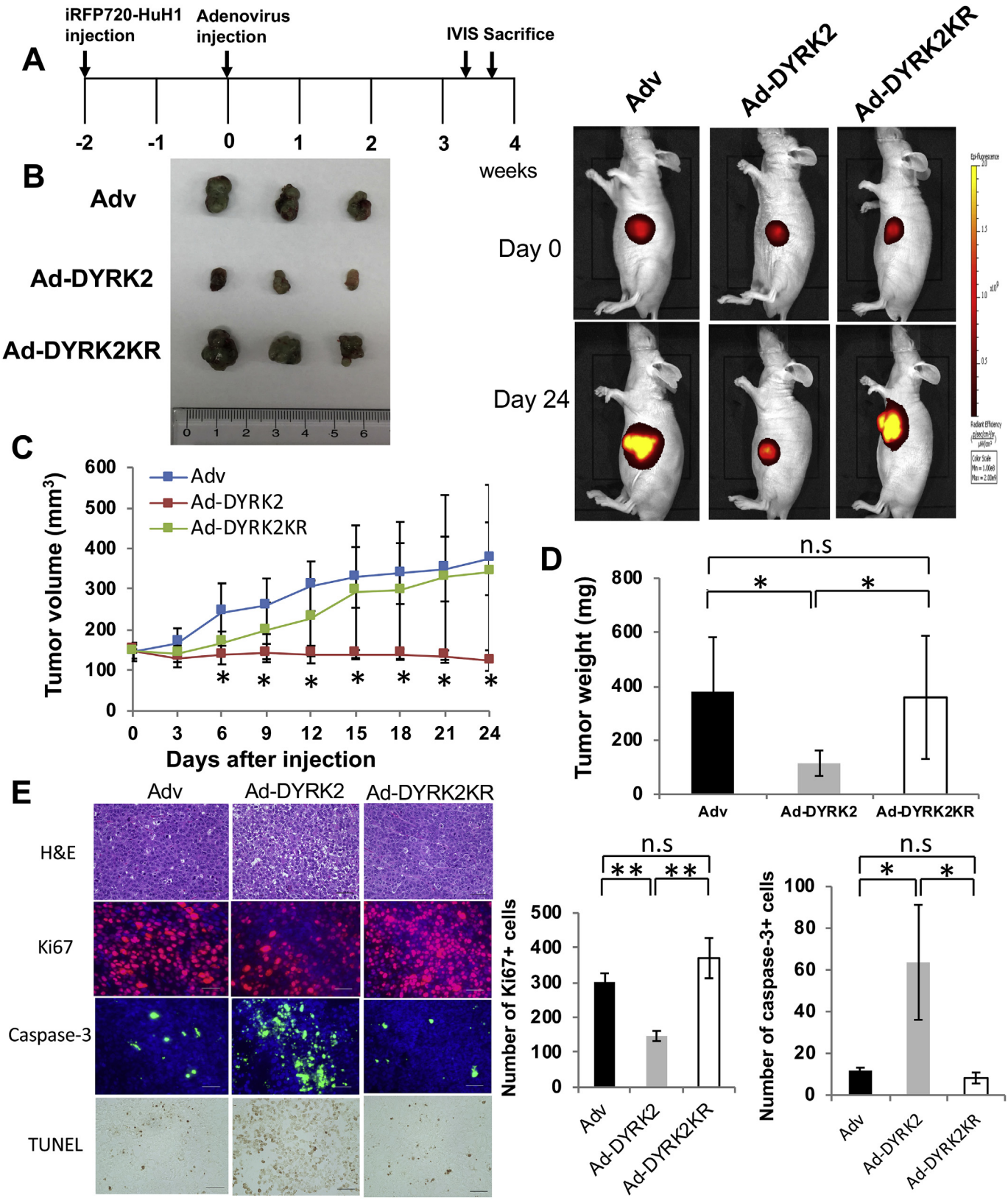

Fig. 4. Ad-DYRK2 inhibited growth and induced apoptosis in HuH1 xenograft tumors. (A) Timeline of the procedure for animal studies. Cells were injected into the subcutaneous space of male nude mice. After two weeks, mice were received multisite intratumor injections with adenovirus encoding DYRK2, DYRK2-KR or empty vector. Tumors were imaged by computed tomography, and near-infrared fluorescent protein (iRFP)-positive cells were examined by an *in vivo* imaging system (n = 5/group). (B) Representative pictures of tumors taken 21 days after adenovirus inoculation. (C) Tumor growth curves were plotted, and xenograft tumor volumes of the recombinant virus groups were compared to the control group. Data are presented as the mean ± SD (Adv n = 5, Ad-DYRK2 n = 5, Ad-DYRK2 -KR n = 5; *p < 0.001). (D) The weight of tumors at 21 days is shown. Data are presented as the mean ± SD (n = 5; *p < 0.05). (E) Enucleated tumors were subjected to staining with H&E, anti-Ki67, anti-caspase 3 or TUNEL. Scale bar: 50 μm (n = 3 mice per group; *p < 0.05, **p < 0.01).

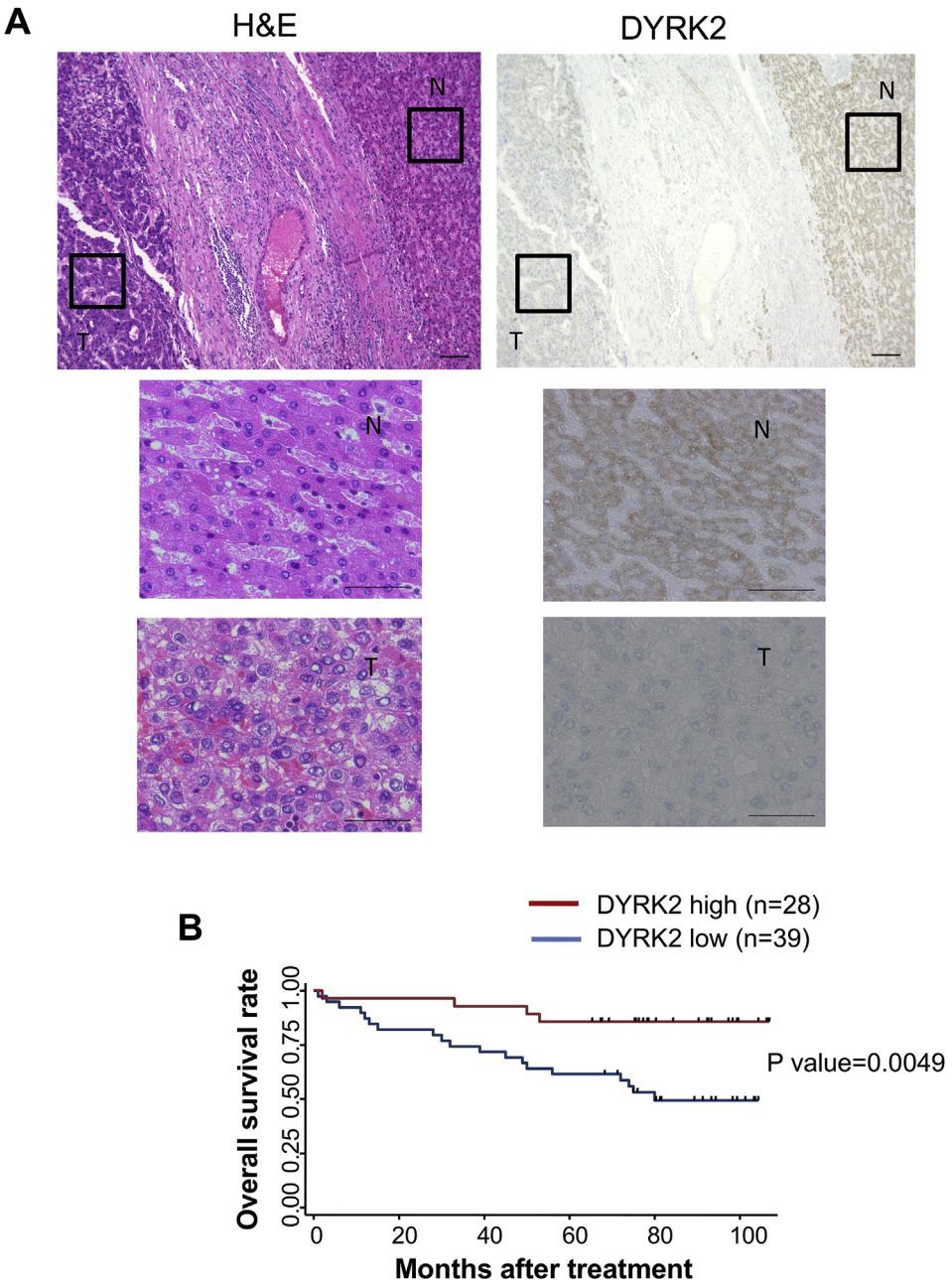

Fig. 5. An immunohistochemical (IHC) analysis of the DYRK2 expression in liver cancer predicted the clinical outcome. (A) An immunohistochemical analysis of the DYRK2 expression in liver cancer and adjacent non-cancerous tissues. (upper) Scale bar: 100 μm; (lower) scale bar: 50 μm. (B) Kaplan–Meier estimates of the overall survival are presented. The groups with high and low expression of DYRK2 were compared. The P values were calculated using the log-rank test.

liver cancer remain obscure. Hence, the present study highlighted the effects of DYRK2 on tumor growth and apoptosis in liver cancer cells. We found that low levels of DYRK2 correlated with cell proliferation, and that DYRK2 over-expressing cells resulted in inhibition of viability, increased the induction of apoptosis, and reduced tumor growth. These findings led us to conduct *in vivo* experiments of tumor formation by forced expression of DYRK2 in anticipation of exploring the potential as one of future therapeutic options.

Adenovirus vectors are widely used in human gene therapy for their efficient and high rate of gene transfer into cells [29–34]. Adenoviruses do not integrate their genes into the genome of the host cells, making these vectors safe and suitable for gene therapy [35]. Of note, we have constructed adenoviruses using the EF1a promoter according to the article by Nakai et al. demonstrating that this promoter induce little if any inflammation or toxicity in the liver [36]. Accumulating evidence has shown that DYRK2 exerts experimental anti-tumor effects on several types of tumors [14,16,27,28]. However, there is no report regarding approaches of therapeutic DYRK2-gene transfer. In the current study, we have demonstrated for the first time that adenovirus-mediated overexpression of DYRK2 exerts an anti-tumor effect in the liver cancer xenograft model. In this context, previous reports have described that tumor enlargement even when adenovirus was administered multiple times with a single gene into the xenograft, and the inhibition of tumor growth was only observed in combination with other genes [35,37]. With respect to anti-tumor effects, Ad-DYRK2 showed markedly decreased tumor growth in nude mice with xenograft tumors without the combined administration of anti-cancer drugs. Importantly, a single administration of Ad-DYRK2 exhibited dramatic anti-tumor effects without multiple dosing. These results provide evidence that the gene transfer of DYRK2 exerts a promising anti-tumor effect and may be

useful as a therapeutic option against liver cancer. Our group and others previously demonstrated that reduced expression of DYRK2 induced chemo-resistance [15,27], suggesting that the combination of Ad-DYRK2 with chemo-drug may induce synergizing effects. We are now planning to conduct experiments in other cancers to assess potential anti-tumor effects by the DRYK2-gene transfer.

Accumulating studies have demonstrated that DYRK2 is down-regulated in various cancer tissues such as breast, lung, colon, prostate, and that low DYRK2 expression is clearly associated with a poor prognosis [14,16,27,28]. The present study confirmed that the levels of DYRK2 correlated with the prognosis in liver cancer patients. Our findings suggest that DYRK2 could be a predictive surrogate indicator of aggressiveness and poor survival in patients with liver cancer.

In conclusion, our findings provide the first evidence that the adenovirus-mediated overexpression of DYRK2 inhibits liver cancer progression. The expression of DYRK2 could be a useful predictive marker for the prognosis. The stabilized or forced expression of DYRK2 may become a potential target for novel gene therapy against liver cancer.

Conflicts of interest

The authors have no conflict of interest.

Acknowledgments

The authors appreciate all patients who provided clinical samples for this study. The authors thank Prof. L. M. Reid for providing RNA of human normal hepatocytes. This work was supported by grants from the Japan Society for the Promotion of Science (KAKENHI Grant Nos. JP26290041, JP17H03584, and JP16K09378), the Jikei University Graduate Research Found, Takeda Science Foundation, Bristol-Myers Squibb foundation and SGH foundation.

Appendix A. Supplementary data

Supplementary data to this article can be found online at https://doi.org/10.1016/j.canlet.2019.02.046.

References

[1] J.M. Llovet, J. Zucman-Rossi, E. Pikarsky, B. Sangro, M. Schwartz, M. Sherman, G. Gores, Hepatocellular carcinoma, Nat. Rev. Dis. Primers 2 (2016) 16018.
[2] H.B. El-Serag, Hepatocellular carcinoma, N. Engl. J. Med. 365 (2011) 1118–1127.
[3] G.A. Michelotti, M.V. Machado, A.M. Diehl, NAFLD, NASH and liver cancer, Nat. Rev. Gastroenterol. Hepatol. 10 (2013) 656–665.
[4] B. Sun, M. Karin, Obesity, inflammation, and liver cancer, J. Hepatol. 56 (2012) 704–713.
[5] J.M. Llovet, S. Ricci, V. Mazzaferro, P. Hilgard, E. Gane, J.F. Blanc, A.C. de Oliveira, A. Santoro, J.L. Raoul, A. Forner, M. Schwartz, C. Porta, S. Zeuzem, L. Bolondi, T.F. Greten, P.R. Galle, J.F. Seitz, I. Borbath, D. Haussinger, T. Giannaris, M. Shan, M. Moscovici, D. Voliotis, J. Bruix, S.I.S. Group, Sorafenib in advanced hepatocellular carcinoma, N. Engl. J. Med. 359 (2008) 378–390.
[6] A.L. Cheng, Y.K. Kang, Z. Chen, C.J. Tsao, S. Qin, J.S. Kim, R. Luo, J. Feng, S. Ye, T.S. Yang, J. Xu, Y. Sun, H. Liang, J. Liu, J. Wang, W.Y. Tak, H. Pan, K. Burock, J. Zou, D. Voliotis, Z. Guan, Efficacy and safety of sorafenib in patients in the Asia-Pacific region with advanced hepatocellular carcinoma: a phase III randomised, double-blind, placebo-controlled trial, Lancet Oncol. 10 (2009) 25–34.
[7] J. Bruix, J.L. Raoul, M. Sherman, V. Mazzaferro, L. Bolondi, A. Craxi, P.R. Galle, A. Santoro, M. Beaugrand, A. Sangiovanni, C. Porta, G. Gerken, J.A. Marrero, A. Nadel, M. Shan, M. Moscovici, D. Voliotis, J.M. Llovet, Efficacy and safety of sorafenib in patients with advanced hepatocellular carcinoma: subanalyses of a phase III trial, J. Hepatol. 57 (2012) 821–829.
[8] A.L. Cheng, Z. Guan, Z. Chen, C.J. Tsao, S. Qin, J.S. Kim, T.S. Yang, W.Y. Tak, H. Pan, S. Yu, J. Xu, F. Fang, J. Zou, G. Lentini, D. Voliotis, Y.K. Kang, Efficacy and safety of sorafenib in patients with advanced hepatocellular carcinoma according to baseline status: subset analyses of the phase III Sorafenib Asia-Pacific trial, Eur. J. Cancer 48 (2012) 1452–1465.
[9] J.L. Raoul, J. Bruix, T.F. Greten, M. Sherman, V. Mazzaferro, P. Hilgard, H. Scherubl, M.E. Scheulen, G. Germanidis, S. Dominguez, S. Ricci, A. Nadel, M. Moscovici, D. Voliotis, J.M. Llovet, Relationship between baseline hepatic status and outcome, and effect of sorafenib on liver function: SHARP trial subanalyses, J. Hepatol. 56 (2012) 1080–1088.
[10] N. Taira, K. Nihira, T. Yamaguchi, Y. Miki, K. Yoshida, DYRK2 is targeted to the nucleus and controls p53 via Ser46 phosphorylation in the apoptotic response to DNA damage, Mol. Cell. 25 (2007) 725–738.
[11] M. Perez, C. Garcia-Limones, I. Zapico, A. Marina, M.L. Schmitz, E. Munoz, M.A. Calzado, Mutual regulation between SIAH2 and DYRK2 controls hypoxic and genotoxic signaling pathways, J. Mol. Cell Biol. 4 (2012) 316–330.
[12] N. Taira, H. Yamamoto, T. Yamaguchi, Y. Miki, K. Yoshida, ATM augments nuclear stabilization of DYRK2 by inhibiting MDM2 in the apoptotic response to DNA damage, J. Biol. Chem. 285 (2010) 4909–4919.
[13] N. Taira, R. Mimoto, M. Kurata, T. Yamaguchi, M. Kitagawa, Y. Miki, K. Yoshida, DYRK2 priming phosphorylation of c-Jun and c-Myc modulates cell cycle progression in human cancer cells, J. Clin. Investig. 122 (2012) 859–872.
[14] R. Mimoto, N. Taira, H. Takahashi, T. Yamaguchi, M. Okabe, K. Uchida, Y. Miki, K. Yoshida, DYRK2 controls the epithelial-mesenchymal transition in breast cancer by degrading Snail, Cancer Lett. 339 (2013) 214–225.
[15] N. Yamaguchi, R. Mimoto, N. Yanaihara, Y. Imawari, S. Hirooka, A. Okamoto, K. Yoshida, DYRK2 regulates epithelial-mesenchymal-transition and chemosensitivity through Snail degradation in ovarian serous adenocarcinoma, Tumour Biol. 36 (2015) 5913–5923.
[16] Y. Enomoto, S. Yamashita, Y. Yoshinaga, Y. Fukami, S. Miyahara, K. Nabeshima, A. Iwasaki, Downregulation of DYRK2 can be a predictor of recurrence in early stage breast cancer, Tumour Biol. 35 (2014) 11021–11025.
[17] N. Bonifaci, B. Gorski, B. Masojc, D. Wokolorczyk, A. Jakubowska, T. Debniak, A. Berenguer, J. Serra Musach, J. Brunet, J. Dopazo, S.A. Narod, J. Lubinski, C. Lazaro, C. Cybulski, M.A. Pujana, Exploring the link between germline and somatic genetic alterations in breast carcinogenesis, PLoS One 5 (2010) e14078.
[18] M. Honda, S. Yogosawa, M. Kamada, Y. Kamata, T. Kimura, Y. Koike, T. Harada, H. Takahashi, S. Egawa, K. Yoshida, A novel near-infrared fluorescent protein, iRFP720, facilitates transcriptional profiling of prostate cancer bone metastasis in mice, Anticancer Res. 37 (2017) 3009–3013.
[19] T. Oikawa, A. Kamiya, M. Zeniya, H. Chikada, A.D. Hyuck, Y. Yamazaki, E. Wauthier, H. Tajiri, L.D. Miller, X.W. Wang, L.M. Reid, H. Nakauchi, Sal-like protein 4 (SALL4), a stem cell biomarker in liver cancers, Hepatology 57 (2013) 1469–1483.
[20] Z. Pei, S. Kondo, Y. Kanegae, I. Saito, Copy number of adenoviral vector genome transduced into target cells can be measured using quantitative PCR: application to vector titration, Biochem. Biophys. Res. Commun. 417 (2012) 945–950.
[21] A. Maekawa, Z. Pei, M. Suzuki, H. Fukuda, Y. Ono, S. Kondo, I. Saito, Y. Kanegae, Efficient production of adenovirus vector lacking genes of virus-associated RNAs that disturb cellular RNAi machinery, Sci. Rep. 3 (2013) 1136.
[22] S. Miyake, M. Makimura, Y. Kanegae, S. Harada, Y. Sato, K. Takamori, C. Tokuda, I. Saito, Efficient generation of recombinant adenoviruses using adenovirus DNA-terminal protein complex and a cosmid bearing the full-length virus genome, Proc. Natl. Acad. Sci. U. S. A. 93 (1996) 1320–1324.
[23] T. Chiyo, S. Sekiguchi, M. Hayashi, Y. Tobita, Y. Kanegae, I. Saito, M. Kohara, Conditional gene expression in hepatitis C virus transgenic mice without induction of severe liver injury using a non-inflammatory Cre-expressing adenovirus, Virus Res. 160 (2011) 89–97.
[24] D. Pei, J. Dai, Y. Kuang, H. Wang, L. Ren, J. Shao, B. Zuo, S. Li, Z. Jiang, M. Li, Effect of influenza A virus non-structural protein 1(NS1) on a mouse model of diabetes mellitus induced by Streptozotocin, Biochem. Biophys. Res. Commun. 419 (2012) 120–125.
[25] D. Ito, S. Yogosawa, R. Mimoto, S. Hirooka, T. Horiuchi, K. Eto, K. Yanaga, K. Yoshida, Dual-specificity tyrosine-regulated kinase 2 is a suppressor and potential prognostic marker for liver metastasis of colorectal cancer, Cancer Sci. 108 (2017) 1565–1573.
[26] C. Yokomizo, K. Yamaguchi, Y. Itoh, T. Nishimura, A. Umemura, M. Minami, K. Yasui, H. Mitsuyoshi, H. Fujii, N. Tochiki, T. Nakajima, T. Okanoue, T. Yoshikawa, High expression of p300 in HCC predicts shortened overall survival in association with enhanced epithelial mesenchymal transition of HCC cells, Cancer Lett. 310 (2011) 140–147.
[27] X. Zhang, P. Xu, W. Ni, H. Fan, J. Xu, Y. Chen, W. Huang, S. Lu, L. Liang, J. Liu, B. Chen, W. Shi, Downregulated DYRK2 expression is associated with poor prognosis and Oxaliplatin resistance in hepatocellular carcinoma, Pathol. Res. Pract. 212 (2016) 162–170.
[28] S. Nomura, Y. Suzuki, R. Takahashi, M. Terasaki, R. Kimata, Y. Terasaki, T. Hamasaki, G. Kimura, A. Shimizu, Y. Kondo, Dual-specificity tyrosine phosphorylation-regulated kinase 2 (DYRK2) as a novel marker in T1 high-grade and T2 bladder cancer patients receiving neoadjuvant chemotherapy, BMC Urol. 15 (2015) 53.
[29] S. Markmann, B.P. De, J. Reid, C.L. Jose, J.B. Rosenberg, P.L. Leopold, S.M. Kaminsky, D. Sondhi, O. Pagovich, R.G. Crystal, Biology of the adrenal gland cortex obviates effective use of adeno-associated virus vectors to treat hereditary adrenal disorders, Hum. Gene Ther. 29 (2018) 403–412.
[30] L.S. Carvalho, R. Xiao, S.J. Wassmer, A. Langsdorf, E. Zinn, S. Pacouret, S. Shah, J.I. Comander, L.A. Kim, L. Lim, L.H. Vandenberghe, Synthetic adeno-associated viral vector efficiently targets mouse and nonhuman primate retina in vivo, Hum. Gene Ther. 29 (2018) 771–784.
[31] T.R. Flotte, Therapeutic advances in Germany and beyond, Hum. Gene Ther. 28 (2017) 1117.
[32] H.L. Gray-Edwards, A.N. Randle, S.A. Maitland, H.R. Benatti, S.M. Hubbard, P.F. Canning, M.B. Vogel, B.L. Brunson, M. Hwang, L.E. Ellis, A.M. Bradbury, A.S. Gentry, A.R. Taylor, A.A. Wooldridge, D.R. Wilhite, R.L. Winter, B.K. Whitlock, J.A. Johnson, M. Holland, N. Salibi, R.J. Beyers, J.L. Sartin, T.S. Denney, N.R. Cox, M. Sena-Esteves, D.R. Martin, Adeno-associated virus gene therapy in a sheep model of tay-sachs disease, Hum. Gene Ther. 29 (2018) 312–326.
[33] Y. Tao, M. Huang, Y. Shu, A. Ruprecht, H. Wang, Y. Tang, L.H. Vandenberghe,

Q. Wang, G. Gao, W.J. Kong, Z.Y. Chen, Delivery of adeno-associated virus vectors in adult mammalian inner-ear cell subtypes without auditory dysfunction, Hum. Gene Ther. 29 (2018) 492–506.
[34] G. Ungerechts, C.E. Engeland, C.J. Buchholz, J. Eberle, H. Fechner, K. Geletneky, P.S. Holm, F. Kreppel, F. Kuhnel, K.S. Lang, M.F. Leber, A. Marchini, M. Moehler, M.D. Muhlebach, J. Rommelaere, C. Springfeld, U.M. Lauer, D.M. Nettelbeck, Virotherapy research in Germany: from engineering to translation, Hum. Gene Ther. 28 (2017) 800–819.
[35] L. Dai, Q. Pan, Y. Peng, S. Huang, J. Liu, T. Chen, X. Wang, D. Chen, J. Wang, Y. Zhu, H. Wang, Y. Liu, Y. Ou, X. Yu, K. Cao, p53 plays a key role in the apoptosis of human ovarian cancer cells induced by adenovirus-mediated CRM197, Hum. Gene Ther. 29 (2018) 916–926.
[36] M. Nakai, K. Komiya, M. Murata, T. Kimura, M. Kanaoka, Y. Kanegae, I. Saito, Expression of pIX gene induced by transgene promoter: possible cause of host immune response in first-generation adenoviral vectors, Hum. Gene Ther. 18 (2007) 925–936.
[37] Q. Luo, H. Liu, Z. Zhang, S. Basnet, Z. Dai, S. Li, Y. Wang, B. Xu, H. Ge, A dual-regulated oncolytic adenovirus carrying TAp63 gene exerts potent antitumor effect on colorectal cancer cells, Am. J. Transl. Res. 9 (2017) 2966–2974.

Forced expression of DYRK2 exerts anti-tumor effects via apoptotic induction in liver cancer cells

Supplementary Figure 1. Stable knockdown of DYRK2 in PLC/PRF5 cells increased proliferation *in vitro*. (A) PLC/PRF5 cells were transfected with shDYRK2#1, shDYRK2#5 or shLuc as control. The expression of DYRK2, c-Myc, Cyclin D1, and Cyclin D2 was analyzed by Western blotting. (B) Cell growth was measured by a CCK-8 assay. Data are presented as the mean ± SD (n = 3; *p<0.01). (C) Cells were stained with propidium iodide, and the cell cycle was analyzed using flow cytometry (*p<0.05, **p<0.01).

Supplementary Figure 2. DYRK2 knockdown increased cell growth *in vivo* in PLC/PRF5 cells. (A) Representative pictures of tumors were taken four weeks after inoculation. (B) Tumor growth curves are plotted for shDYRK2 #5 and shLuc cells. Data are presented as the mean ± SD (n = 5; *p<0.01). (C) The weight of the tumor at four weeks is shown. Data are expressed as the mean ± SD (n = 5; *p<0.01).

Supplementary Figure 3. The adenovirus-mediated overexpression of DYRK2 in HuH1

cells. (A) The expression of DYRK2 was higher in normal human hepatocytes than that in liver cancers. (B) A schematic representation of adenoviruses encoding DYRK2 (Ad-DYRK2), kinase-dead mutant (K178R) of DYRK2 (Ad-DYRK2-KR) or an empty vector as control (Adv). (C) Analysis of DYRK2 expression with different MOIs by western blotting. (D) Cell growth was measured by the CCK-8 assay. Data are presented as the mean ± SD (n = 3; *p<0.05, **p<0.01). (E) Cell growth was measured by the colony formation assay.

Supplementary Figure 4. The adenovirus-mediated overexpression of DYRK2 in PLC/PRF5 cells. (A) PLC/PRF5 cells were infected with Ad-DYRK2, Ad-DYRK2-KR, or Adv. The expression of DYRK2 was analyzed by Western blotting. (B) Cell growth was measured by a CCK-8 assay. Data are presented as the mean ± SD (n = 3; *p<0.01). (C) Cells were stained with propidium iodide, and the cell cycle was analyzed using flow cytometry (*p<0.05, **p<0.01).

Supplementary Figure 5. The expression levels of DYRK2 in liver cancer tissues. (A) Representative example of DYRK2 immunohistochemistry in liver tumors. Negative (IHC score 0); weak (IHC score 1); moderate (IHC score 2); strong (IHC score 3). Cytoplasmic

staining of DYRK2 was divided into two groups: a low-expression group (including negative and weak categories, score 0 or 1), and a high-expression group (including moderate and strong categories, score 2 or 3). Scale bars represent 50 μm.

Supplementary Figure 1

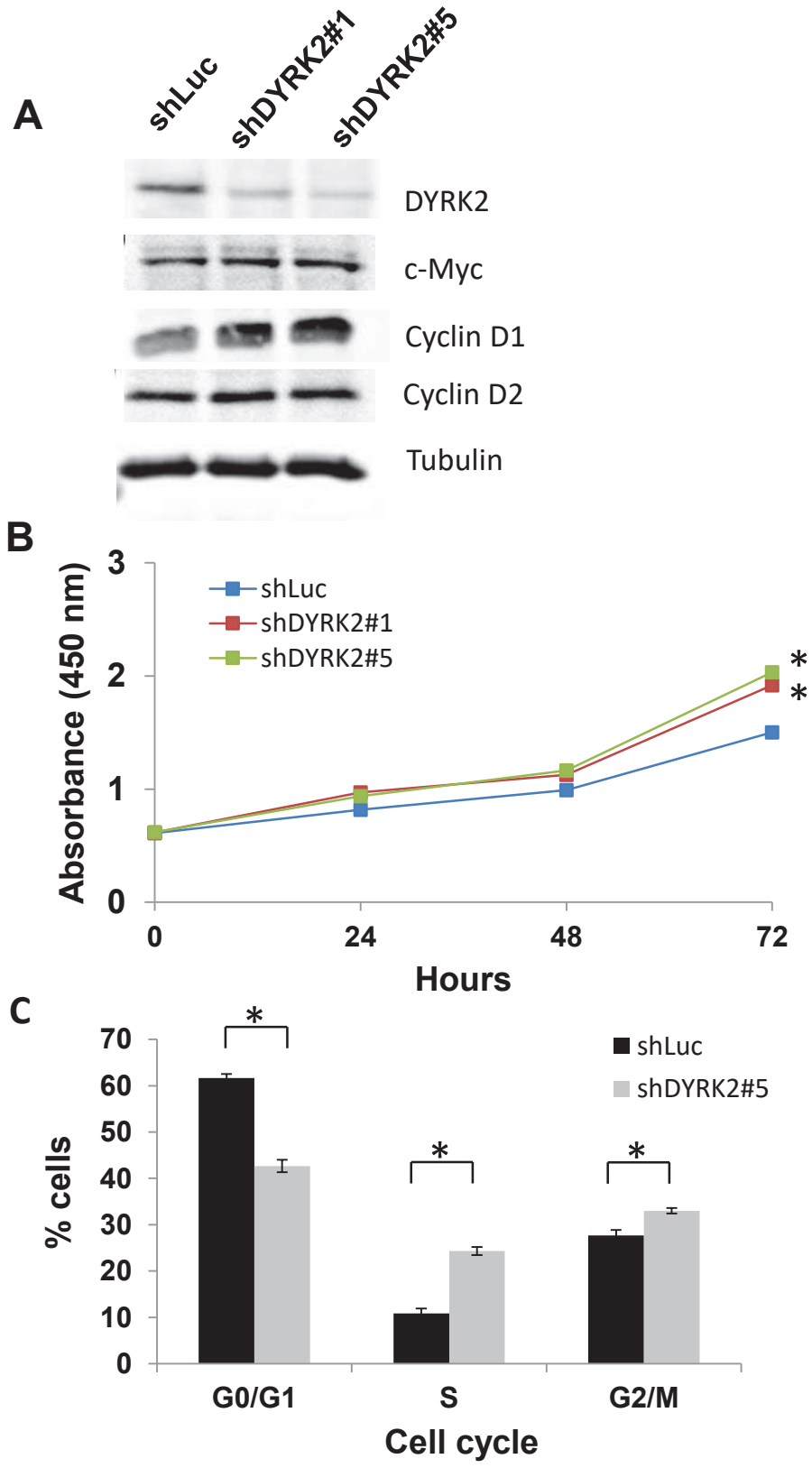

Supplementary Figure 2

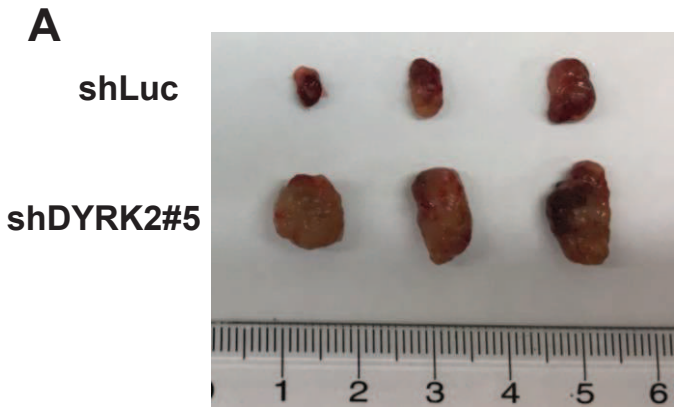

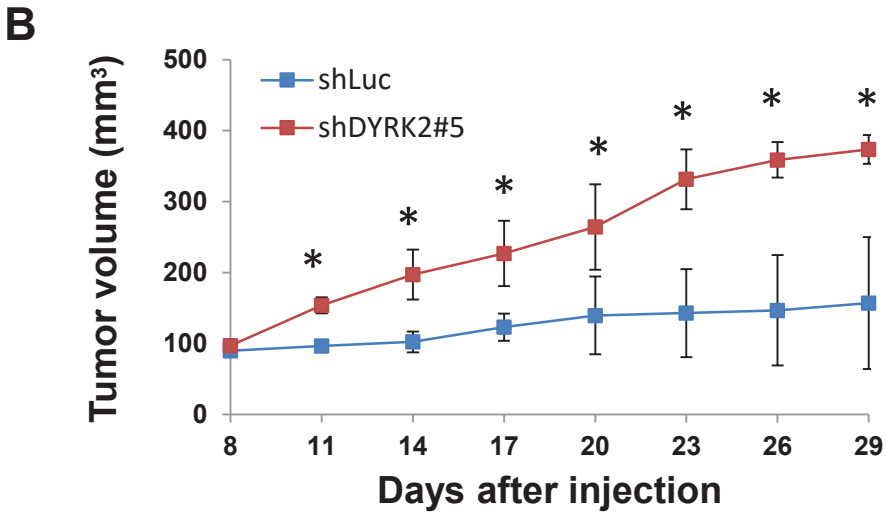

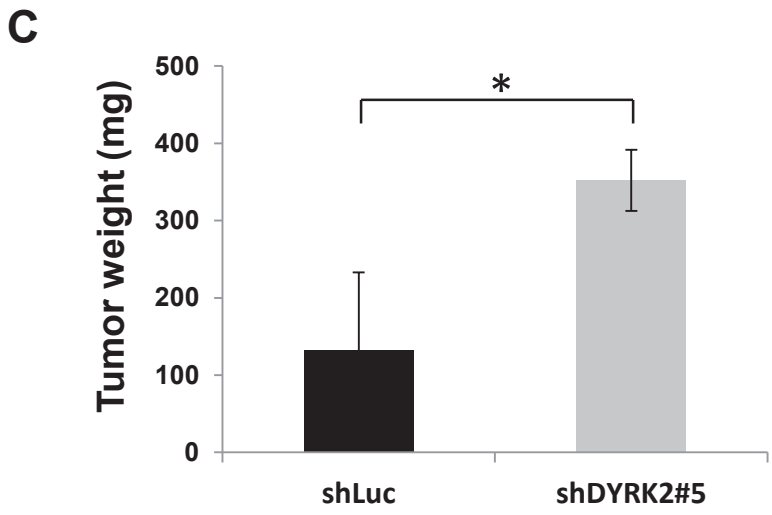

Supplementary Figure 3

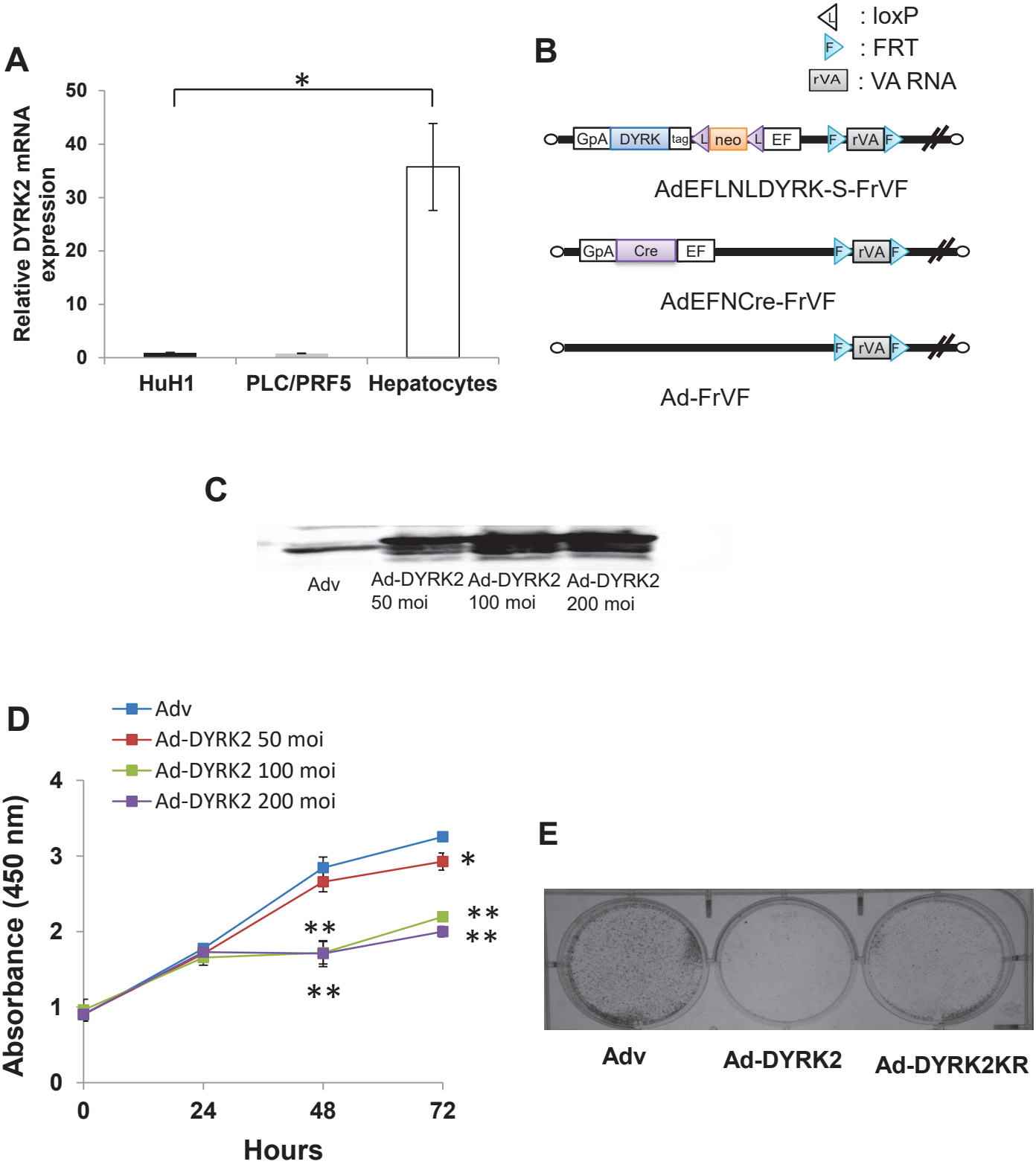

Supplementary Figure 4

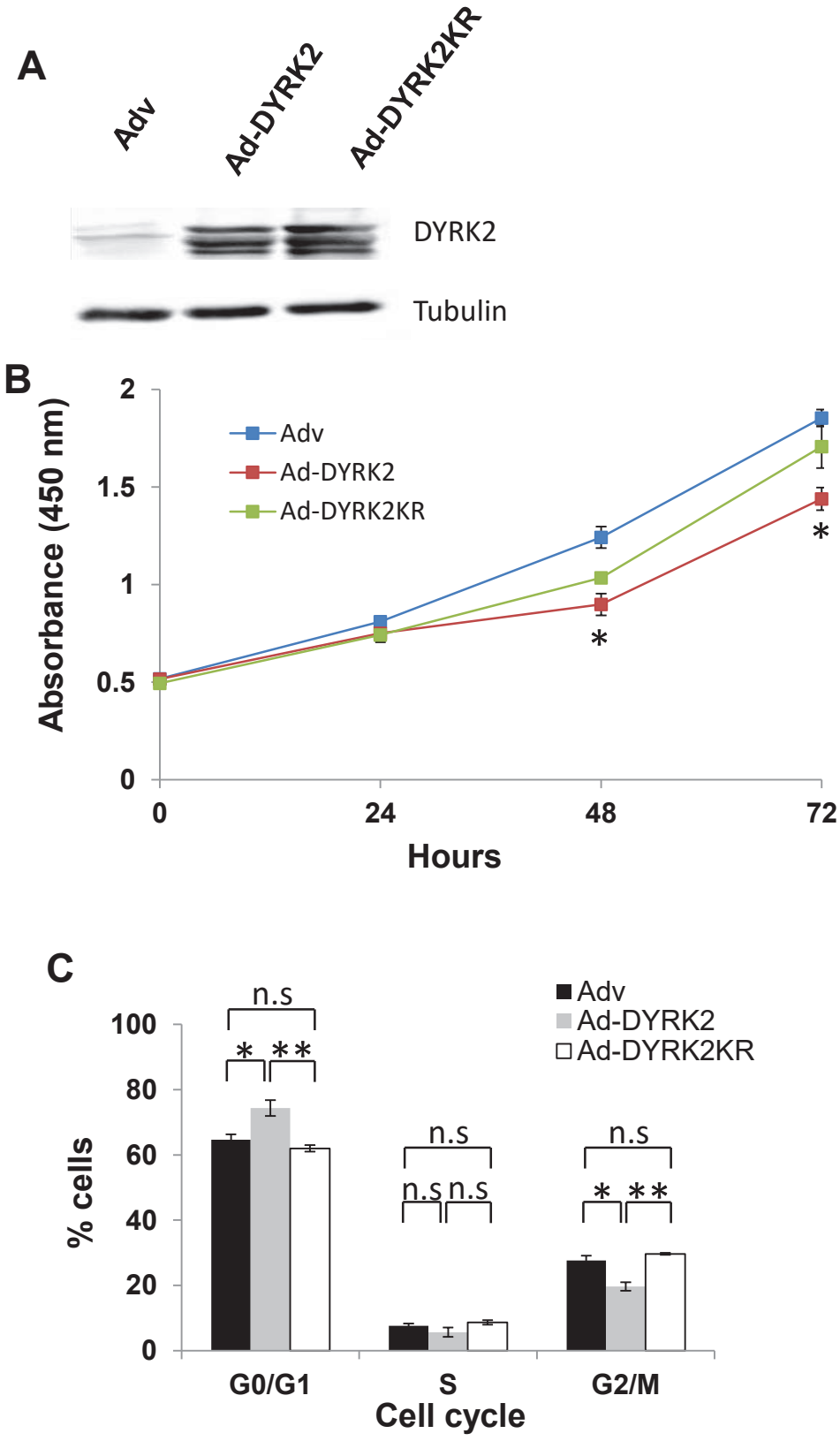

Supplementary Figure 5

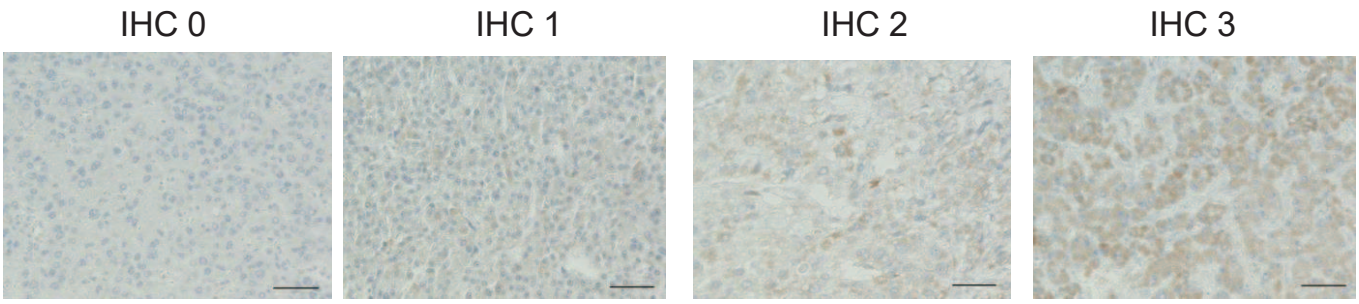

Supplementary Table 1. The correlation between DYRK2 and the pathological characteristics of liver cancer.

	All (n=67)	**DYRK2-High HCC (n=28)**	**DYRK2-Low HCC (n=39)**	***p*-value**
Mean age (years)				
≤64	30	12	18	0.79
>64	37	16	21	
Gender				0.99
Male	55	23	32	
Female	12	5	7	
Tumor size (cm)				0.86
≤5	51	21	30	
>5	16	7	9	
Liver cirrhosis				0.024
Absent	37	20	17	
Present	30	8	22	
Tumor number				0.87
1	52	22	30	
≥2	15	6	9	
Vascular invasion				0.69
Absent	51	22	29	
Present	16	6	10	
Tumor differentiation				0.53
Well-	17	6	11	
Moderately/Poorly	50	22	28	
TNM stage				0.53
I, II	45	20	25	
III, IV	22	8	14	

Supplementary Table 2. Factors associated with the overall survival in a multivariable analysis.

	Hazard ratio	95% CI	*p*-value
Mean age (years) ≤64 >64	2.74	1.07- 6.96	0.035
Gender Male Female	0.21	0.02 -1.78	0.15
Tumor size (cm) ≤5 >5	2.42	1.02-5.73	0.045
Liver cirrhosis Absent Present	0.65	0.25-1.66	0.37
Tumor number 1 ≥2	1.81	0.60-5.44	0.29
Vascular invasion Absent Present	2.17	0.61-7.80	0.23
Tumor differentiation Well-Moderately/Poorly	0.58	0.21-1.60	0.29
TNM stage I, II III, IV	1.92	0.50-7.34	0.34
DYRK2 High Low	0.24	0.08-0.71	0.01

Supplementary Table 3. Primer sequences.

Primer for subcloning

piRFP720-N1	Forward	GGGGGATCCGCCACCATGGCGGAAGGATCCGTCGC
	Reverse	GGGGAATTCTCACTCTTCCTACACGCCGAT

Primers for quantitative real-time polymerase chain reaction

DYRK2	Forward	TCAAGGCTGAGAACGGGAAG
	Reverse	ATGGTGGTGAAGACGCCAGT
GAPDH	Forward	GGGGAGAAAACGTCAGTGAA
	Reverse	TCTGCGCCAAATTAGTCCTC

Supplementary Table 4. Sequences of shRNA.

shRNA DYRK2#1	5’-GATCCCCTCACGTGGCTTACAGGTATTTCAAGAGAATACCT GTAAGCCACGTGATTTTTA-3’
shRNA DYRK2#5	5’-GATCCCCACTCACAGCCTTCGAACACTTCAAGAGAGTGTTC GAAGGCTGTGAGTTTTTTGGAAA-3’

Supplementary Table 5. Comparison of DYRK2 expression between tumor regions and non-tumor regions in each patient tissue (n = 67).

	DYRK2			
	High	**Low**	***p*-value**	**Equal**
Tumor regions compared to non-tumor regions	4	52	<0.001	12